Histone citrullination as a novel biomarker and target to inhibit progression of abdominal aortic aneurysms

WOLF EILENBERG, BRANISLAV ZAGRAPAN, SONJA BLEICHERT, NAHLA IBRAHIM, VIKTORIA KNÖBL, ANNIKA BRANDAU, LUCA MARTELANZ, MARIE-THERESE GRASL, HUBERT HAYDEN, PAIMANN NAWROZI, RENATA RAJIC, CHARLOTTE HÄUSLER, ALEXANDROS POTOLIDIS, NAWA SCHIRWANI, ANDREAS SCHEUBA, JOHANNES KLOPF, PETER TEUBENBACHER, MARKUS P. WEIGL, PATRICK KIRCHWEGER, DIETRICH BEITZKE, ALEXANDER STIGLBAUER-TSCHOLAKOFF, ADELHEID PANZENBÖCK, IRENE LANG, LISA-MARIE MAURACHER, LENA HELL, INGRID PABINGER, MARC A. BAILEY, D. JULIAN A. SCOTT, LARS MAEGDEFESSEL, ALBERT BUSCH, IHOR HUK, CHRISTOPH NEUMAYER, and CHRISTINE BROSTJAN

VIENNA, AUSTRIA; LEEDS, UNITED KINGDOM; MUNICH, GERMANY; AND STOCKHOLM, SWEDEN

Neutrophil extracellular traps (NETs) have been implicated in the pathogenesis of abdominal aortic aneurysms (AAAs). This study has addressed the notion that NET components might serve as AAA biomarkers or novel targets of AAA therapy. Thus, parameters of neutrophil activation and NET formation were measured in plasma. Their diagnostic marker value was explored in 41 AAA patients and 38 healthy controls. The NET parameter citrullinated histone H3 (citH3) was then validated in 63 AAA patients and 63 controls matched for cardiovascular disease. The prognostic marker potential was investigated in 54 observation periods of AAA growth over 6 months. NETs were further assessed in conditioned medium and sections of aortic tissue. CitH3 was found to be increased in blood (median 362 vs 304 ng/mL, $P = 0.004$) and aortic tissue (50 vs 1.5 ng/mg, $P < 0.001$) of AAA patients compared to healthy controls and accumulated in the intraluminal thrombus (629 ng/mg). The diagnostic potential of citH3 ranged at 0.705 area under the ROC curve (AUROC) and was validated with the independent sample set. Furthermore, plasma citH3 predicted AAA growth over the next 6 months (AUROC: 0.707, $P = 0.015$) and dropped significantly after surgical aneurysm repair. In an angiotensin II - based mouse model of experimental AAA, an inhibitor of histone citrullination was applied to

From the Department of General Surgery: Division of Vascular Surgery, Medical University of Vienna, Vienna, Austria; Department of Biomedical Imaging and Image Guided Therapy: Division of Cardiovascular and Interventional Radiology; Division of Molecular and Gender Imaging, Medical University of Vienna, Vienna, Austria; Department of Internal Medicine II: Division of Cardiology, Medical University of Vienna, Vienna, Austria; Department of Internal Medicine I: Clinical Division of Haematology and Haemostaseology, Medical University of Vienna, Vienna, Austria; Leeds Institute of Cardiovascular and Metabolic Medicine, University of Leeds, Faculty of Medicine and Health, Leeds, United Kingdom; Leeds Vascular Institute, Leeds General Infirmary, Leeds, United Kingdom; Department of Vascular and Endovascular Surgery, Klinikum rechts der Isar, Technical University Munich, Munich, Germany; Molecular Vascular Medicine Group, Centre for Molecular Medicine, Karolinska Institute, Stockholm, Sweden.

Submitted for Publication November 29, 2020; received submitted January 31, 2021; accepted for publication February 4, 2021.

Reprint requests: Christine Brostjan, Department of General Surgery, Division of Vascular Surgery, Medical University of Vienna, Anna Spiegel Centre for Translational Research, Vienna General Hospital 25.05.002, A-1090 Vienna, Austria. e-mail: christine.brostjan@meduniwien.ac.at.

1931-5244/$ - see front matter

https://doi.org/10.1016/j.trsl.2021.02.003

block NET formation and AAA progression. Of note, further growth of an established aneurysm was prevented in mice treated with the NET inhibitor ($P = 0.040$). In conclusion, histone citrullination represents a promising AAA biomarker and potential therapeutic target to control disease progression. (Translational Research 2021; 233:32–46)

Abbreviations: AAA = abdominal aortic aneurysm; AngII = angiotensin II; AUROC = area under the receiver operating curve; BMI = body mass index; citH3 = citrullinated histone H3; COPD = chronic obstructive pulmonary disease; CTA = computed tomography angiography; ELISA = enzyme-linked immunosorbent assay; IL-1β = interleukin 1 beta; ILT = intraluminal thrombus; MMP = matrix metalloproteinase; MPO = myeloperoxidase; NET = neutrophil extracellular trap; NGAL = neutrophil-gelatinase associated lipocalin; PADI4 = peptidyl arginine deiminase 4; PBS = phosphate-buffered saline

AT A GLANCE COMMENTARY

Eilenberg W, et al

Background

NETs are known to play a role in the pathogenesis of AAA and the central NET component of histone citrullination is detectable in aneurysm tissue.

Translational Significance

In a clinical investigation, plasma citH3 showed diagnostic marker value and potential to predict rapid AAA expansion. Thus, citH3 might serve as companion biomarker (in addition to established imaging methods) to noninvasively monitor AAA growth. Proof-of-concept for targeting histone citrullination to block AAA progression has been provided in a mouse model. Considering the current lack of conservative treatment options, this constitutes an attractive approach for AAA drug development with expectedly few side-effects.

INTRODUCTION

Progressive dilatation of an abdominal aortic aneurysm (AAA) may lead to its rupture, which is associated with a death rate of around 80%.[1] Whilst current evidence supports surgical repair of asymptomatic AAAs at a diameter of 5 to 5.5 cm, autopsy studies have shown that small AAAs may also rupture.[2] Therefore, it is of primary importance that already small asymptomatic aneurysms are diagnosed in patients and adequately managed. Until now, mainly ultrasound imaging and computed tomography angiography (CTA) are used to monitor diameter changes and to assess the risk of AAA rupture.[1] Regarding biomarkers, D-dimer proved to be significantly elevated in blood of AAA patients and has prognostic power despite its limited specificity.[3,4]

Besides the progressive weakening and widening of the vessel wall, development of an intraluminal thrombus (ILT) can further promote aneurysmal dilatation.[5] Among other leukocytes, neutrophils are recruited to the aortic wall as well as the ILT and substantially contribute to AAA development, since neutrophil-derived serine proteases, matrix metalloproteinases (MMPs) and reactive oxygen species induce matrix destruction and promote smooth muscle cell apoptosis.[6] We have recently reported that the frequency of activated neutrophils and neutrophil-derived myeloperoxidase (MPO) are significantly elevated in blood of AAA patients compared to healthy controls and have investigated the diagnostic and prognostic value of a score based on MPO and D-dimer plasma levels.[4] Of note, neutrophil depletion inhibits AAA formation in mice. This effect is partly mediated by a decrease in MMP activity but additional neutrophil functions also seem to be involved.[7]

Excessive neutrophil activation can lead to the formation of neutrophil extracellular traps (NETs) proposed to immobilize and destroy pathogens.[8] These web-like structures are composed of discharged chromatin, histones, elastase, myeloperoxidase (MPO), MMP-9 and other neutrophil proteins. Expulsion of chromatin requires partial DNA decondensation, which is primarily achieved by histone modifications such as citrullination via the peptidyl arginine deiminase 4 (PADI4) enzyme.[9] Apart from the antimicrobial defence, NETs are also involved in the pathogenesis of diseases such as cancer or autoimmune conditions. In thrombosis, the concomitant recruitment of platelets and neutrophils promotes NET formation and the subsequent activation of the extrinsic and intrinsic coagulation pathways.[10] NETs were also discovered in the luminal part of the ILT and the aortic adventitia of AAA patients, and were initially proposed to be triggered by periodontal bacteria found at the aneurysm site.[11] However, NETs were also detected in a mouse model of sterile AAA development where interleukin 1 beta (IL-1β) was shown to trigger NET formation.[12]

NETs were found to recruit and activate plasmacytoid dendritic cells resulting in the secretion of interferon alpha, thereby propagating the local immune reaction at the aneurysm site.[13] NET inhibition or application of DNase I was successful in reducing AAA formation when administered early on during experimental aneurysm induction.[12-14]

Considering these initial reports, we devised the hypothesis that NET parameters may have diagnostic or prognostic marker value for AAA patients. In addition, NET blockade might have a therapeutic potential and serve to limit the progression of established disease. To address these hypotheses, we analysed the hallmarks of neutrophil activation and parameters of NET formation, such as citrullinated histone H3 (citH3) in AAA patients as compared to matched control subjects and assessed their diagnostic potential in an exploration and validation cohort. Furthermore, we analysed these plasma markers at 6-month intervals to determine their prognostic value. To verify that NET markers originate from the AAA site we investigated resected aneurysm tissue and compared plasma parameters before and after surgery. The effect of NET blockade on AAA progression was tested using a specific inhibitor of histone citrullination in mouse models of established AAA.

METHODS

Ethics statement. All studies involving human subjects were conducted according to The Code of Ethics of the World Medical Association (Declaration of Helsinki), were reviewed and approved by the local ethics committee and informed consent was obtained from the study participants.

Diagnostic study design (explorative cohort). As approved by the institutional ethics committee of the Medical University of Vienna (Ref 1729/2014) AAA patients under surveillance at the Vienna General Hospital were enrolled between January 2014 and December 2016. Patient demographics were recorded by a structured questionnaire, blood plasma was collected and all study subjects underwent a CTA scan. A group of advanced AAA patients scheduled for surgical repair (N = 41) was matched in sex, age, body mass index (BMI) and smoking habit with healthy volunteers (N = 38) subjected to ultrasound examination for absence of AAA. The exclusion criteria for patients and controls were recent (<1 year) tumour and/or chemotherapy, systemic autoimmune or haematological disease and organ transplantation.

For a subset of AAA patients (N = 28) who underwent aneurysm repair by either open surgery (N = 14) or endovascular procedure (N = 14) a second blood sample was processed within 3−13 months after the intervention to compare pre- and postoperative parameter levels.

Diagnostic validation cohort. For the validation set citrated plasma samples of 63 AAA patients and 63 controls from the Leeds Aneurysm Development Study (Leeds General Infirmary, approved by the Leeds East Ethics Committee, Ref 03/142)[15] were included. All subjects underwent ultrasound examination for AAA diagnosis. Patients and controls were matched one-to-one based on sex, age (within 2 years) and the presence of cardiovascular disease (composite of: previous myocardial infarction, angina pectoris, peripheral vascular disease or cerebrovascular disease).

Prognostic study design. Based on the above-mentioned study approval by the institutional ethics committee of the Medical University of Vienna (Ref 1729/2014) and the listed inclusion and exclusion criteria, we enrolled 28 asymptomatic AAA patients in a longitudinal observation study from 2014 to 2019 at the Surgery Department of the Medical University of Vienna. We performed a total of 54 monitoring cycles with serial blood drawing and CTA analysis at baseline and every 6 months thereafter.

CTA was performed using a Siemens Somatom Flash or Somatom Force device (Siemens Healthineers, Erlangen, Germany) with tube voltage settings of 120 or 100 kV and a tube current of 120 ref mAs. Collimation was 2 × 64 × 0.6 mm. Images are reconstructed in 1 and 3 mm slices, and 1 mm slices are used for multiplanar reconstructions. The data are analysed with the CT vascular module of syngo.via (Siemens Healthineers). The software is designed to automatically identify the centre line of the aorta and align orthogonal views of the aortic cross-section. The AAA maximum diameter is measured with semi-automatic tools with mean intra- and interobserver variability ranging at 0.13 mm and 0.27 mm, respectively.

Measurement of plasma factors. Peripheral, human venous blood was drawn into prechilled citrate, theophylline, adenosine, dipyridamole containing tubes (Greiner Bio One, Kremsmünster, Austria) for processing within 60 minutes of collection as previously described.[16] Platelet-free plasma was obtained by centrifugation of whole blood at 1,000 x g and subsequently at 10,000 x g at 4˚C for 10 minutes and stored in aliquots at -80˚C.

The neutrophil and NET parameters MPO (BioTechne, Minneapolis, MN, USA), circulating cell-free DNA-histone complexes (Cell Death Detection Kit, Roche, Basel, Switzerland), citH3[17] and IL-1β (Thermo Fisher Scientific, Waltham, MA, USA) were measured by ELISA. The mean coefficient of variation

for the citH3 ELISA ranged at 6% (SD = 8.9%) for duplet measurements. Neutrophil-gelatinase associated lipocalin (NGAL) and elastase were assayed by the Human Sepsis Magnetic Bead Panel 3 (EMD Millipore Corp., Billerica, MA, USA) in a Luminex MagPix instrument (Thermo Fisher Scientific).

The serum lipid profile, clinical parameters of haemostasis, inflammation, and kidney function were assessed by the Vienna General Hospital central laboratory.

Angiotensin II-induced AAA formation in *ApoE* null mice. The animal experiments were approved by the local ethics committee and the Austrian Ministry of Science (BMWFW-66.009/0355-WF/V/3b/2016 and 0248-WF/V/3b/2017), conforming to the European Directive 2010/63/EU (on the protection of animals used for scientific purposes) and the Austrian Animal Experiment Act 2012.

Male mice homozygous for the *ApoE* mutation (B6.129P2-Apoe^{tm1Unc}/J@Him), aged 10−15 weeks and kept on normal diet, received angiotensin II (AngII, Bachem, Bubendorf, Switzerland) at 1000 ng/kg/min by subcutaneously implanted ALZET 2004 osmotic pumps (DURECT Corp., Cupertino, CA, USA) over 28 days.[18] Measurements of AAA volume were conducted by ultrasound on day 9 and mice were stratified 1:1 to treatment groups accordingly (N = 8 per group). On day 10, vascular access mini-ports (VAB 1 channel 22ga, Instech Laboratories Inc., Plymouth Meeting, PA, USA) were inserted subcutaneously and the external jugular vein was cannulated. Mice received either PBS (phospate-buffered saline) or PBS containing 0.2 μg PADI4 inhibitor GSK484 (Cayman Chemical, Ann Arbor, MI, USA) in a volume of 10 μL/g mouse weight per day via mini-port from day 10 to 28.[9]

For ultrasound measurements of aneurysms, the following settings of the Vevo 2100 Imaging System (FUJIFILM VisualSonics Inc., Toronto, ON, Canada) were applied: gain 30 dB, image depth 9 mm, image width 8.08 mm. Respiratory gating was set to 25% delay and a window of 50%; T1 50 ms were used for ECG trigger. After localization of the left renal artery, the MS550 transmitter was moved 6 mm cranially for automated scan of the suprarenal aorta. 157 imaging frames were generated over a scan distance of 12 mm with 0.076 mm step size. The suprarenal aortic volume was calculated in mm^3 (over the monitored distance of 12 mm) with Vevo Lab 3.1.1 software; images of ECG-gated kilohertz visualization were used to additionally determine the maximum diameter of the aorta (inner-to-inner wall) at maximal blood flow.[19] Independent measurements by 3 observers were averaged in volume and diameter calculations.

Prior to ultrasound measurement or surgery, animals were anesthetized with 3% isoflurane, 2 L/min O_2. Once the animals were fully sedated, they were kept under reduced anaesthesia at 1.8%−2% isoflurane, 2 L/min O_2 for the entire procedure. Before surgeries, the animals were injected subcutaneously with 0.05 mg/kg buprenorphine. Post intervention, the animals received 10 μL/g of 10% glucose subcutaneously and recovered under a heat lamp at 37°C. Until the 3rd postoperative day, mice were given piritramide and glucose in drinking water (7.5 mg piritramide and 20 mL 5% glucose in 200 mL 0.9% NaCl).

Elastase-induced AAA formation in black 6 wild-type mice. As approved by the Austrian authorities (2020-0.547.895) male C57BL6/J mice aged 9 to 11 weeks, received topical periadventitial elastase application to the infrarenal aorta to induce AAA formation: The mice underwent open median laparotomy and the infrarenal portion of the aorta was separated from surrounding fat and connective tissue, creating a unilateral periaortic pouch where 10 μL of porcine pancreatic elastase (Sigma-Aldrich, St. Louis, MO, USA) at 7.6 mg/mL were applied for 5 minutes. The elastase was absorbed with a cotton swab and the abdomen flushed 3 times with saline before closure. On day 5, the vascular access mini-ports were implanted and daily injections of GSK484 at 0.4 μg in a volume of 10 μL/g mouse weight (N = 5) or PBS (N = 5) were administered until day 13. The aortic volume was monitored by 3D ultrasound (as specified above) at baseline, and day 4 (for stratification of mice to treatment groups) and day 13 after elastase application. However, since aneurysms develop infrarenally in this model, the MS550 transmitter was moved 6 mm caudally from the left renal artery for an automated scan of the infrarenal aorta. On day 14, aortas were excised and subjected to ex vivo measurement of maximal diameter by 2 observers; results were averaged.

Analysis of conditioned media from aortic tissue. Aortic wall and intraluminal thrombus were collected during open surgical AAA repair; control aorta samples were obtained from sex-matched transplant donors (Ref 1729/2014). Small (3 × 3 × 3 mm) pieces were fresh-frozen in liquid nitrogen and stored at -80°C. RPMI-1640 medium supplemented with antibiotics was added to thawed tissue samples at 6 mL medium per gram of tissue (wet weight) and incubated at 37°C for 24 hours.[11] Afterwards the conditioned medium was centrifuged (3,000 x g for 10 minutes at room temperature) and assayed for MPO or citH3 by ELISA. Comparably, citH3 levels were determined in conditioned medium from mouse aortas harvested on day 29 after aneurysm treatment with 2 μg/g/d GSK484 (vs PBS control) from day 14-28.

Immunofluorescence analysis of NETs in tissue sections. Tissue samples of healthy aortic wall, AAA wall or AAA thrombus (Ref 1729/2014) were formalin fixed, paraffin embedded and 5 μm sections were subjected to antigen retrieval in citrate buffer, then permeabilized and stained with mouse antihuman CD66b antibody (clone 80H3, Immunotech/Beckman Coulter, Brea, CA, USA) at 2 μg/mL and with polyclonal rabbit antihuman citH3 antibody (ab5103, Abcam, Ltd., Cambridge, United Kingdom) at 1 μg/mL. Alexa Fluor 647 goat antimouse IgG and Alexa Fluor 555 donkey antirabbit IgG were applied at 1:1000 as secondary reagents; DNA was stained with Hoechst 33342 at 1:1000 working dilution (all Thermo Fisher Scientific). Tissue image acquisition was performed at 20-fold magnification utilizing an automated Axio Observer Z1 microscope (Carl Zeiss MicroImaging, Inc., Oberkochen, Germany) and the TissueFAXS scan software (TissueGnostics GmbH, Vienna, Austria). Automated image analysis was conducted with TissueQuest software (version 4.0.1.01040, TissueGnostics GmbH). CD66b+ neutrophils, negative or positive for citH3, were determined per mm^2 of tissue. The fraction (permille) of tissue area staining positive for citH3 was also analysed to quantitate the extent of NET formation. For better tissue visualization, autofluorescence detection of elastin and collagen fibres in the FITC channel was included. In a limited sample set, sections were costained for human myeloperoxidase by goat polyclonal IgG (AF3667, Bio-Techne) at 2.5 μg/mL.

For the analysis of NETs in resected mouse aorta, paraffin sections were comparably stained with rat antimouse Ly6G (clone 1A8, BioLegend, San Diego, CA, USA) at 1:1000 working dilution as well as rabbit polyclonal anti-citH4 antibody (07-596, Merck KGaA, Darmstadt, Germany) at 1:500 dilution. Please note that anti-citH4 antibody was applied in stainings of mouse tissue due to better species reactivity than the anti-citH3 antibody; both histones are subject to citrullination by PADI4. The matching secondary antibodies Cy3 donkey antirat IgG (Dianova, Barcelona, Spain) and Alexa Fluor 647 donkey antirabbit IgG (Thermo Fisher Scientific) were applied at 1:400 dilution, while the DNA dye Hoechst 33342 was included at 1:1000. Consecutive tissue sections were subjected to staining with haematoxylin and eosin for comparison. Mounted samples were analysed with an LSM780 confocal microscope (Carl Zeiss MicroImaging, Inc.).

Immunofluorescence analysis of NETs in mouse blood smears. Mouse blood was harvested from the inferior *vena cava* and supplied with ethylene diamine tetraacetic acid for anticoagulation. To trigger NET formation by PADI4 activation, increasing doses of the calcium ionophore A23187 (200, 500, 1000 μM) were supplied to 25 μL of whole blood and incubated at 37˚C for 2 hours prior to blood distribution on a glass slide. Slides were kept frozen at -80˚C until fixation, permeabilization and immunostaining with rabbit polyclonal anti-citH4 antibody (Merck) at 1:300 dilution. Alexa Fluor Plus 555 donkey antirabbit IgG (Thermo Fisher Scientific), Alexa Fluor 488 rat antimouse Ly6G antibody (BioLegend) both at 1:300 and Hoechst 33342 DNA dye at 1:10,000 working dilution were applied in a second staining step. Mounted samples were analysed at 200-fold magnification with an Axio Observer Z1 fluorescence microscope (Carl Zeiss MicroImaging, Inc.) in combination with the TissueFAXS software (6.0.6245.103, TissueGnostics). Images were analysed using StrataQuest software (6.0.1.140) for automated detection of double (Hoechst/Ly6G) and triple (Hoechst/Ly6G/citH4) positive cells to deduce the percentage of NETosing neutrophils among all detected neutrophils. Scanned regions of interest were chosen to cover a minimum of 100 analysed neutrophils.

Statistical analysis. Data of human samples are given as median values and interquartile range (IQR). Nonparametric tests were used for group comparisons (Mann-Whitney U or Wilcoxon signed-rank test) or correlations (Spearman r). Contingency tables, chi-square or Fisher's exact test (for expected counts below 5) were applied for categorical variables. Receiver operating characteristics (ROC) analysis served to evaluate the diagnostic and prognostic marker potential by the area under the ROC curve (AUROC). Multivariable analysis (binary logistic regression, method Enter) was conducted to assess the diagnostic value of plasma citH3 for AAA in relation to co-morbidities and medication. In the prognostic setting, slow vs fast disease progression was defined as <2 or ≥ 2 mm increase in AAA diameter over 6 months matching previously published cut-offs at 4 mm per year.[20]

For mice (stratified to treatment groups based on AAA volume of day 9) data were expressed in % growth of aneurysm volume compared to baseline (mean and standard error). Normal data distribution was verified by Shapiro-Wilk test and hence statistical group comparison was performed by paired T-test for day 28.

Analyses were conducted with SPSS 25.0 software (IBM, Armonk, NY, USA) and a significance level of $P < 0.05$ was applied.

DATA AVAILABILITY STATEMENT

The data underlying this article will be shared on reasonable request to the corresponding author.

RESULTS

Plasma levels of citH3 have diagnostic marker value for AAA. In an exploratory study design, 41 AAA patients scheduled for surgical repair were compared to 38 healthy controls, matched for age, sex, smoking habit und BMI (Table 1). The maximum aortic diameter of AAA patients ranged between 44 and 114 mm (median 57 mm; Suppl. Table 1). The 2 groups were found to differ in demographic variables known to be associated with AAA and cardiovascular disease. Patients showed a higher incidence of hypertension, hyperlipidaemia and pertaining medication, chronic obstructive pulmonary disease (COPD) and coronary heart disease, which was also reflected in an elevated Framingham Risk Score. In line with previous studies, the fibrin degradation product D-dimer was significantly increased in the blood of AAA patients compared to controls (median 1.30 vs 0.47 μg/mL, $P < 0.001$).

Plasma samples were assessed for circulating markers of neutrophil activation (degranulation) such as MPO, NGAL and neutrophil elastase. They were compared to parameters of NET release, specifically cell-free DNA-histone complexes and citH3. Elastase was increased in patient vs control blood at a moderate significance level (5.0 vs 3.7 ng/mL, $P = 0.037$), while MPO (13.3 vs 7.7 ng/mL, $P < 0.001$) and citH3 (362 vs 304 ng/mL, $P = 0.004$) showed highly significant elevations. NGAL and DNA-histone complexes did not differ between groups (Suppl. Table 2, Fig 1A-C). The neutrophil origin of citH3 was suggested by the correlation (Suppl. Table 3, Fig 1D-F) with the neutrophil activation markers MPO ($r = 0.720$, $P < 0.001$) and elastase ($r = 0.493$, $P < 0.001$). Also, neutrophil blood count correlated weakly with circulating citH3 ($r = 0.240$, $P = 0.037$), MPO ($r = 0.271$, $P = 0.018$) and with elastase ($r = 0.442$, $P < 0.001$).

To assess whether the NET parameter citH3 is affected by comorbidities more prevalent in the AAA vs control group, we evaluated plasma citH3 levels according to co-morbidity, but found no significant difference between individuals with and without hypertension, hyperlipidaemia or COPD in our study cohort (Suppl. Table 4). There was a trend towards higher circulating citH3 levels for individuals with coronary heart disease (367 vs 309 ng/mL, $P = 0.062$) and significantly elevated citH3 plasma values for study participants on antiplatelet (354 vs 290 ng/mL, $P = 0.005$) or lipid-lowering therapy (354 vs 306 ng/mL, $P = 0.008$) which was statin-based in all cases, with only 2 AAA patients and 1 healthy control additionally receiving ezetimibe. Importantly, citH3 (along with antiplatelet treatment, hyperlipidaemia or lipid-lowering therapy) proved an independent diagnostic parameter for AAA in multivariable regression analysis (Table 2). Since plasma MPO showed a high correlation with circulating citH3, the 2 biomarkers did not hold independent biomarker information and MPO levels were not included in the multivariable analysis.

Furthermore, an independently established validation set of plasma samples was investigated derived from 63 AAA patients matched with control individuals on a 1:1 basis for age, sex and pre-existing cardiovascular disease (Suppl. Table 5). While citH3 showed a diagnostic marker potential, that is, an AUROC value of 0.705 ($P = 0.004$) in the exploration setting (Fig 2A-C), with a moderate additive value to D-dimer (AUROC of D-dimer: 0.830 vs AUROC of combined model: 0.844), its diagnostic power was still significant but substantially lower in the validation cohort (Fig 2D-F) matched for cardiovascular co-morbidity (AUROC of 0.589, $P = 0.038$). Similar to the exploration set, the validation cohort (AAA vs controls) differed significantly in blood lipids, D-dimer levels, hypertension and antihypertensive as well as lipid-lowering (statin based) and antiplatelet (aspirin) therapy (Suppl. Table 5). In multivariable regression analysis based on the validation cohort (Table 3) citH3 was confirmed as independent diagnostic AAA indicator along with smoking and hypertension or antihypertensive therapy.

Plasma citH3 exhibits prognostic marker potential. In a longitudinal observation study, 28 AAA patients were followed at 6-month intervals with repeated blood analyses and CTA (Suppl. Table 6). A total of 54 monitoring periods was evaluated for baseline citH3 to predict aneurysm growth over the next 6 months. The prognostic value of citH3 ranged at AUROC=0.707 ($P = 0.015$) and was superior to D-dimer (AUROC=0.613, $P = 0.186$) in this setting (Fig 3A-D). Since larger aneurysms are known to be associated with a faster expansion rate[1], we additionally expressed AAA growth as a function of the baseline diameter and obtained comparable results (Suppl. Figure 1).

Based on Youden's index a cut-off level was defined at 194 ng/mL plasma citH3 and found to predict rapid progression ($\geq$ 2 mm/6 months) with 77% sensitivity und 64% specificity. In line, AAA patients with a citH3 plasma level above the median have an odds ratio of 3.94 (95%CI 1.15−13.58) for rapid progression, while individuals within the 4th quartile compared to the 1st quartile exhibit an odds ratio of 8.25 (95%CI 1.15−59.00).

CitH3 drops in circulation after AAA repair and is readily detected in resected tissue. To gather further proof that circulating citH3 is indeed originating from the aneurysm, plasma levels were compared in 28 patients immediately before surgical repair and 3−13 months

Table 1. Patient and control demographics

Characteristic	Healthy (N = 38) *Median (Range)*	AAA (N = 41) *Median (Range)*	*P*-value
Age (years)	67 (39–83)	71 (52–83)	0.705
Body mass index (kg/m^2)	26.2 (20.7–40.1)	28.4 (17.8–34.1)	0.370
	N (%)	***N (%)***	
Sex			
Female	5 (13.2%)	3 (7.3%)	0.390
Male	33 (86.8%)	38 (92.7%)	
Smoker status			
Never	8 (21.1%)	4 (9.8%)	0.160
Past	13 (34.2%)	22 (53.7%)	
Current	16 (42.1%)	14 (34.1%)	
Unknown	1 (2.6%)	1 (2.4%)	
Hypertension	23 (60.5%)	34 (82.9%)	0.026
Antihypertensive therapy	23 (60.5%)	33 (80.5%)	0.051
Hyperlipidaemia	11 (28.9%)	27 (65.9%)	0.001
Lipid-lowering therapy	6 (15.8%)	34 (82.9%)	<0.001
Peripheral artery disease			
No	34 (89.5%)	32 (78.0%)	0.250
Yes	4 (10.5%)	7 (17.1%)	
Unknown	0 (0.0%)	2 (4.9%)	
Coronary heart disease	4 (10.5%)	14 (34.1%)	0.012
Myocardial infarction	3 (7.9%)	9 (22.0%)	0.082
Stroke	3 (7.9%)	3 (7.3%)	0.236
Antiplatelet therapy	12 (31.6%)	36 (87.8%)	<0.001
Diabetes mellitus	4 (10.5%)	9 (22.0%)	0.171
COPD	5 (13.2%)	13 (31.7%)	0.050
AAA family history			
No	34 (89.5%)	34 (82.9%)	0.236
Yes	4 (10.5%)	4 (9.8%)	
Unknown	0 (0.0%)	3 (7.3%)	
	Median (IQR)	***Median (IQR)***	
White blood cells ($\times 10^6$/L)	5650 (2100)	6400 (2190)	0.114
Neutrophils ($\times 10^6$/L)	3375 (1535)	3742 (1350)	0.217
C-reactive protein (mg/dl)	0.26 (0.46)	0.40 (0.43)	0.075
D-dimer (μg/mL)	0.47 (0.49)	1.30 (1.68)	< 0.001
Triglycerides (mg/dl)	121 (73)	141 (59)	0.070
Total cholesterol (mg/dl)	198 (23)	170 (60)	0.037
LDL - cholesterol (mg/dl)	119 (47)	93 (71)	0.171
HDL - cholesterol (mg/dl)	54 (25)	50 (17)	0.030
FRS (risk factors)	0.86 (1.37)	1.13 (0.95)	0.064
FRS (%)	22.9 (23.8)	30.4 (25.7)	0.026
Creatinine (mg/dl)	0.94 (0.22)	1.02 (0.45)	0.059
Blood urea nitrogen (mg/dl)	15.1 (4.1)	17.8 (6.4)	0.001
eGFR (mL/min/1.73m^2)	84.7 (20.0)	76.0 (38.7)	0.045

AAA, abdominal aortic aneurysm; COPD, chronic obstructive pulmonary disease; eGFR, estimated glomerular filtration rate; FRS, Framingham risk score; HDL, high-density lipoprotein; IQR, interquartile range; LDL, low-density lipoprotein.

(median 6 months) after the intervention (Fig 4A-D). Plasma citH3 normalized to levels found in healthy controls upon surgical intervention (median 383 vs 290 ng/mL). Comparable trends were observed for both, open surgery (N = 14) and endovascular repair (N = 14). This decrease was more pronounced for the NET marker citH3 (P = 0.001) than the neutrophil activation marker MPO (P = 0.023). To screen for potential confounders which might account for the postoperative drop in plasma citH3, we evaluated the available routine blood parameters. Of note, patient medication regarding hyperlipidaemia, hypertension and coagulopathy were continued after surgical AAA repair as established prior to intervention. In line, there was no difference in the pre-/postoperative lipid profile, levels of blood cell counts, creatinine, urea, fibrinogen or C-reactive protein (data not shown). Free haemoglobin and blood albumin levels were significantly decreased in the postoperative monitoring period (P = 0.008 and P = 0.041,

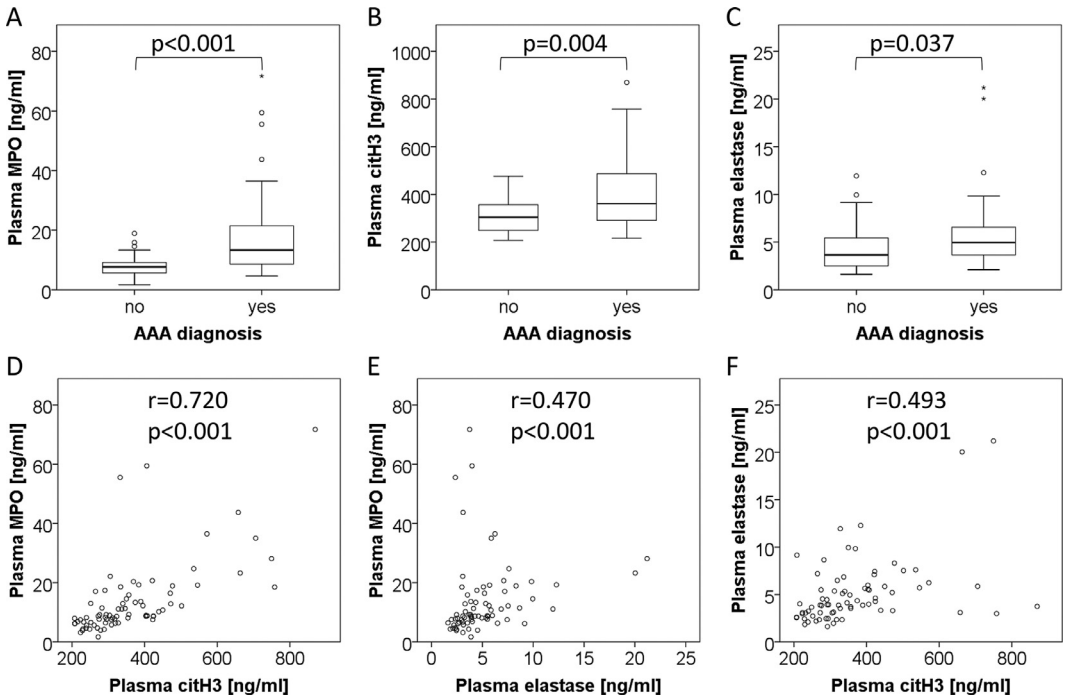

Fig 1. Neutrophil activation and NET parameters in plasma of AAA patients and healthy controls.

Plasma samples of 41 AAA patients and 38 matched controls were analysed for (A) MPO, (B) citH3 and (C) neutrophil elastase (boxplot illustrations, Mann-Whitney U test). Correlations between (D) MPO and citH3, (E) MPO and elastase as well as (F) citH3 and elastase were characterised by scattergrams and Spearman coefficient.

respectively) but did not correlate with plasma citH3 levels.

The resected tissue from AAA patients (aortic wall and ILT) was assessed for citH3/NET content by 2 distinct methods. First, fresh-frozen tissue was immersed in culture medium and the released components were measured in the conditioned medium by ELISA (Suppl. Table 2, Fig 5A-F). The comparison of 27 AAA walls and 27 ILT specimens with 27 controls (aorta samples from sex-matched transplant donors)

Table 2. Multivariable analysis (binary logistic regression, method *Enter*) of AAA diagnosis in the exploration set

Parameter	Exp(B)	95% CI Lower value	95% CI Upper value	*P*-value
Plasma citH3 (ng/mL)	1.011	1.002	1.020	0.020
Age (years)	0.950	0.858	1.051	0.319
Sex	2.605	0.104	65.077	0.560
Smoking	2.368	0.187	30.013	0.506
Hypertension or Antihypertensive therapy‡	2.780	0.187	41.358	0.458
Hyperlipidaemia or lipid-lowering therapy‡	18.414	2.458	137.930	0.005
Peripheral artery disease	0.290	0.036	2.335	0.245
Coronary heart disease	4.290	0.196	94.104	0.355
Myocardial infarction	0.062	0.002	2.058	0.120
Stroke	0.533	0.042	6.685	0.626
Antiplatelet therapy	8.639	1.315	56.753	0.025
COPD	3.494	0.540	22.608	0.189
Constant	0.007			0.231

CI, confidence interval; citH3, citrullinated histone H3; COPD, chronic obstructive pulmonary disease; Exp(B), odds ratio.
‡Due to substantial overlap between co-morbidity and pertaining medication, a combined variable was introduced to avoid issues of collinearity.

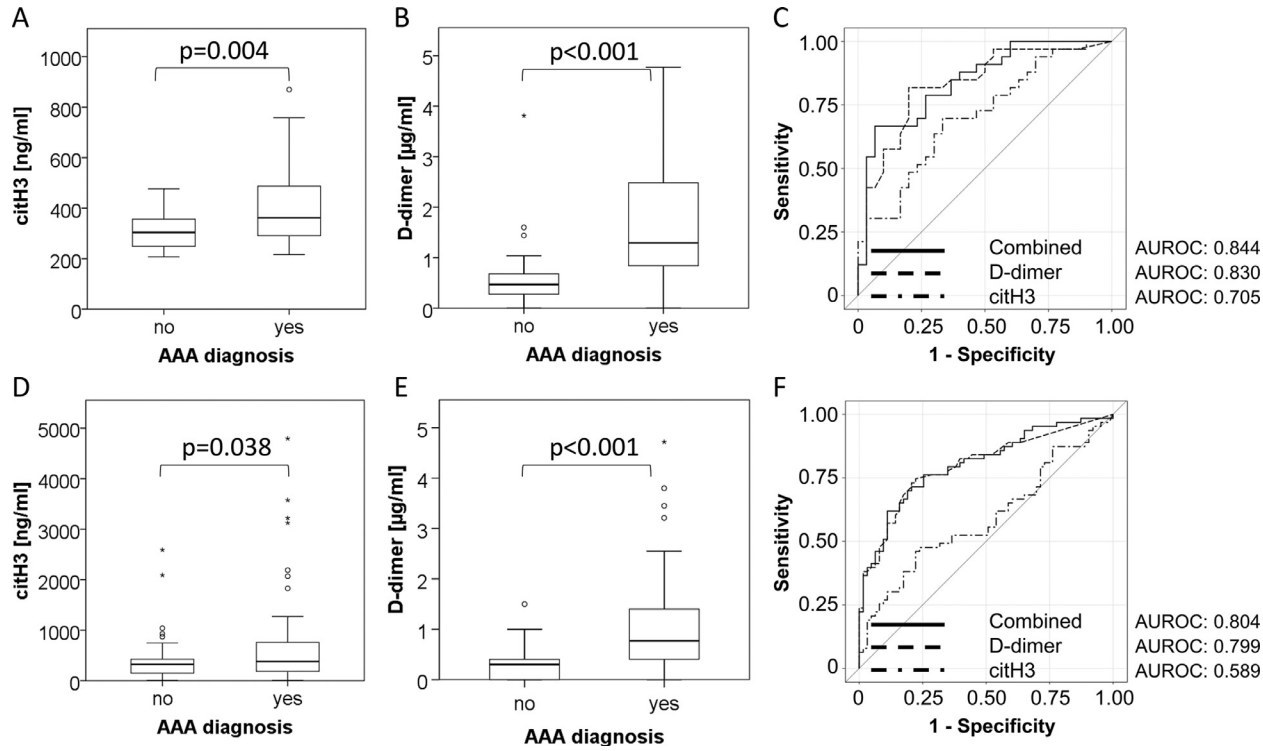

Fig 2. Diagnostic marker value of citH3.

The diagnostic marker potential was evaluated with an (A-C) exploration set and (D-F) validation set of plasma samples: (A) citH3 and (B) D-dimer values in the exploration set of 41 AAA patients and 38 healthy controls (Mann-Whitney U test), (C) AUROC analysis of citH3, D-dimer or combined values for the exploration set. (D) citH3 and (E) D-dimer plasma concentrations in the validation set of 63 AAA patients and 63 controls 1:1 matched for age, sex and cardiovascular disease (Wilcoxon signed-rank test), (F) AUROC analysis of citH3, D-dimer or combined values for the validation set.

revealed that markers of neutrophil activation and NET formation were essentially absent from healthy vessels, while being highly enriched in aneurysm walls and ILT. Levels of citH3 ranged at a median of 1.5 ng/mg tissue in control aortas, at 50 ng/mg in AAA wall ($P < 0.001$ vs healthy) and 629 ng/mg in ILT ($P = 0.002$ vs AAA wall). IL-1β, which was reported to trigger NET formation in AAA mouse models[12], was investigated

Table 3. Multivariable analysis (binary logistic regression, method *Enter*) of AAA diagnosis in the validation set

Parameter	Exp(B)	95% CI Lower value	95% CI Upper value	*P*-value
Plasma citH3 (ng/mL)	1.001	1.000	1.003	0.035
Age (years)	0.932	0.845	1.028	0.162
Sex	2.378	0.308	18.343	0.406
Smoking*	4.848	1.171	20.065	0.029
Hypertension or Antihypertensive therapy*‡	26.074	3.152	215.714	0.002
Lipid-lowering statin therapy*	5.368	0.870	33.105	0.070
Peripheral artery disease*	1.782	0.248	12.799	0.566
Angina pectoris*	0.327	0.010	10.993	0.533
Myocardial infarction*	0.474	0.091	2.481	0.377
Stroke*	10.528	0.576	192.544	0.112
Antiplatelet aspirin therapy*	0.621	0.141	2.723	0.527
Constant	0.224			0.694

CI, confidence interval; citH3, citrullinated histone H3; Exp(B), odds ratio.

‡Due to substantial overlap between co-morbidity and pertaining medication, a combined variable was introduced to avoid issues of collinearity. Please note that the demographic information for parameters marked by asterisk (*) was only available for a limited set of healthy controls (N = 41–44) and AAA patients (N = 41–46).

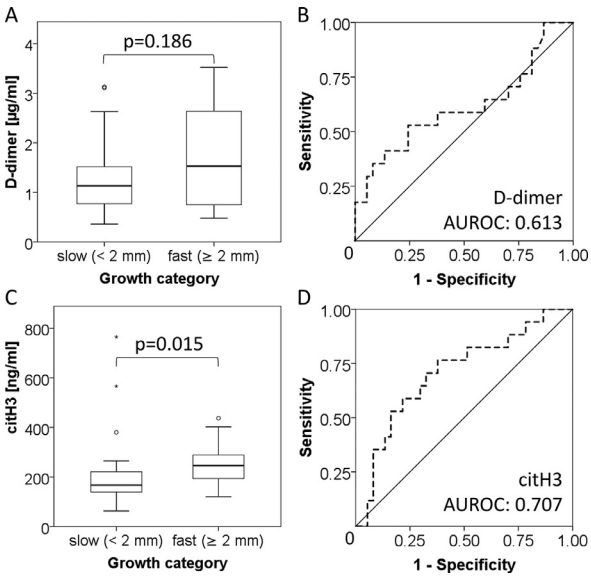

Fig 3. Prognostic marker value of citH3.

To assess the prognostic marker potential, 54 monitoring periods over 6 months were conducted with baseline measurements of (A,B) plasma D-dimer and (C,D) citH3 in AAA patients. Aneurysm growth (in mm of maximal aortic diameter) was determined by CTA at 6 months vs baseline, and was grouped into slow (< 2 mm) and fast (≥ 2 mm) progression. (A,C) Boxplot illustration (Mann-Whitney U test); note: an extreme value is excluded in graph A to enhance plot resolution. (B,D) AUROC analysis.

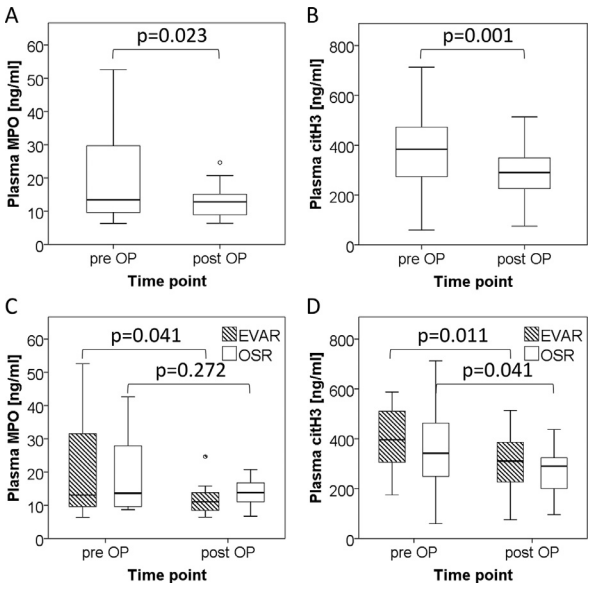

Fig 4. Normalisation of neutrophil and NET parameters after surgical aneurysm repair.

Plasma levels of (A,C) MPO and (B,D) citH3 were compared (A, B) before and after surgery (N = 28) and (C,D) between treatment options (OSR: open surgery, N = 14; EVAR: endovascular repair, N = 14). Boxplot illustration (Wilcoxon signed-rank test); note: an extreme value is excluded in graphs A and C to enhance plot resolution.

in a limited number of samples (N = 13/13/13) and found to be elevated in AAA walls but not in the ILT (Fig 5C). However, it was undetectable in patient plasma (data not shown). All 3 investigated parameters (citH3, MPO and IL-1β) in conditioned medium of the aortic wall showed significant correlations (Suppl. Table 7, Fig 5D-F). Second, paraffin sections were stained for neutrophils and citH3 and subjected to automated analysis by TissueQuest (Fig 6A-G). Both, citH3 negative and citH3 positive neutrophils were highly abundant in AAA tissue as compared to healthy control aorta ($P < 0.001$), with a prevalence of NETosing neutrophils. In contrast to the analysis of tissue-conditioned medium, the total NET area (per-mille of citH3 positive tissue area) was lower in the ILT than in the aneurysm wall (Fig 6F, $P = 0.039$), but was significantly enriched in the luminal vs abluminal layer of the ILT (Fig 6G). To substantiate the neutrophil origin of extracellular traps, costaining for MPO, CD66b and citH3 was conducted for a limited sample set and confirmed that expelled citrullinated histones largely co-localized with MPO (Suppl. Fig 2).

Inhibition of histone citrullination can block disease progression in a mouse model of AAA induced by angiotensin II. The therapeutic potential of targeting histone citrullination was addressed in an animal model of aortic dissection and aneurysm formation triggered by angiotensin II administration to *ApoE*-deficient mice. Ultrasound measurements of suprarenal aortic volume were compared between baseline and day 9 to verify established disease and to stratify mice to treatment groups. On day 10, a mini-port was implanted into the external jugular vein for daily administration of GSK484, a selective PADI4 inhibitor and NETosis blocker in human and murine neutrophils.[9] While 8 mice received the inhibitor from day 10 to 28, 8 control animals were treated with PBS. On day 29, aneurysms and blood were harvested. Mice which had received the PADI4 inhibitor showed a severely impaired capacity of their blood neutrophils to undergo NETosis upon *ex vivo* challenge with a calcium ionophore (Fig 7C, $P = 0.037$). Importantly, the ultrasound investigations revealed that aneurysms stopped to progress in GSK484 treated animals but continued to enlarge in PBS control mice (Fig 7A,B; $P = 0.040$). In line, the tissue levels of citrullinated histones were significantly lower in aneurysms of GSK484 vs PBS treated animals (Fig 7D-F, $P = 0.023$). While GSK484 was successful in limiting aneurysm growth in the angiotensin-II based mouse model, GSK484 administration failed to block disease progression in a second mouse model of AAA induced by periadventitial application of pancreatic porcine elastase despite the presence of citrullinated histones at treatment start (Suppl. Fig 3).

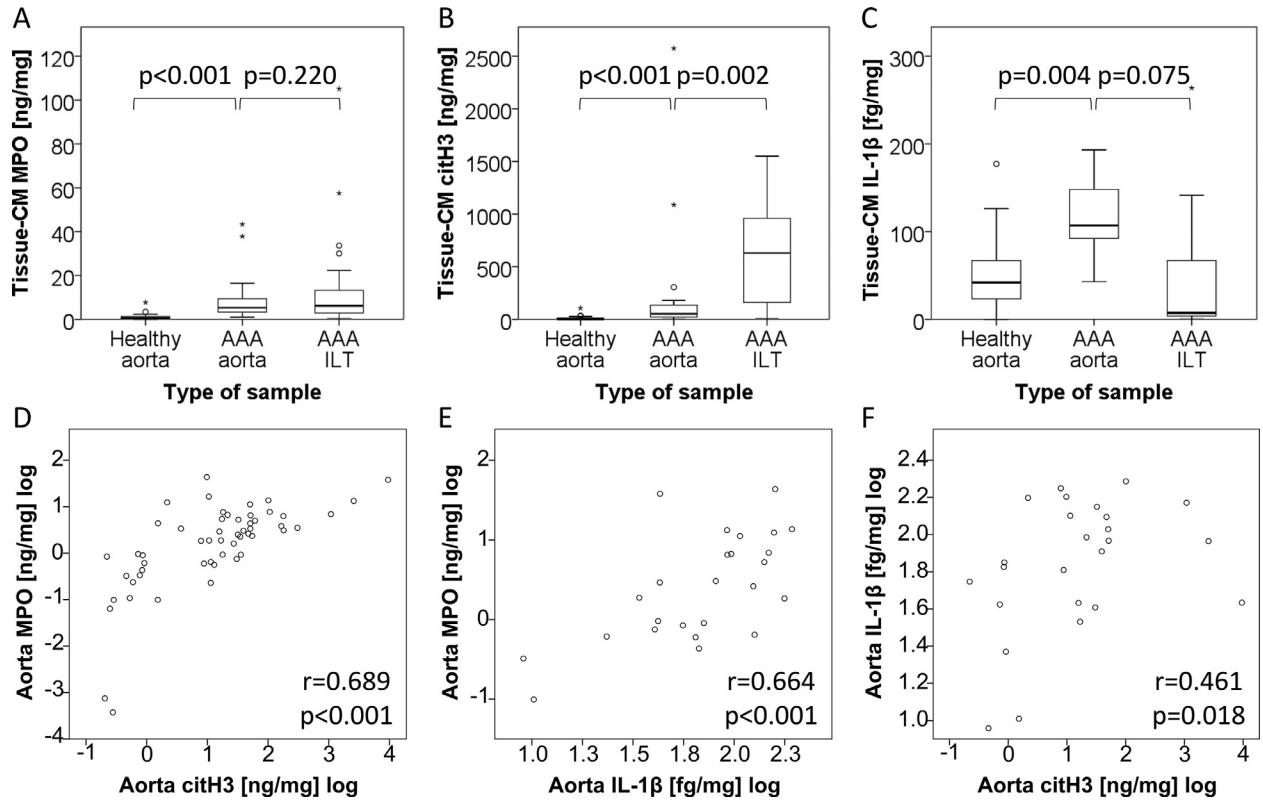

Fig 5. Neutrophil and NET parameters in tissue-conditioned medium of AAA patients and controls.

Tissue-conditioned medium (Tissue-CM) was generated from resected AAA walls, ILT and control aortas from transplant donors. N = 27/27/27 samples were investigated for (A) MPO and (B) citH3, while N = 13/13/13 were assessed for (C) IL-1β content by ELISA [Mann-Whitney U test (healthy vs AAA aorta); Wilcoxon signed-rank test (AAA aorta vs ILT)]. Correlations between (D) MPO and citH3, (E) MPO and IL-1β as well as (F) citH3 and IL-1β were characterised by Spearman coefficient (for combined data of AAAs and healthy aortas). Please note that data were log10-transformed for better illustration by scattergram; extreme values were omitted from graph B to enhance plot resolution.

DISCUSSION

The diagnostic marker value of circulating citH3 for AAA. This study has addressed the clinical potential of NET parameters, in particular citrullinated histones, as biomarkers of AAA. Previous studies have documented the presence of NET components in blood and tissue of AAA patients.[11,12] Regarding blood analyses, NET detection was focused on circulating cell-free DNA or MPO-DNA complexes in human plasma.[11] About 20% of plasma DNA was found to be associated with MPO which renders circulating, free DNA a rather unspecific and insensitive biomarker of NET formation. This is reflected in our plasma measurements of DNA-histone complexes which did not differ significantly between AAA patients and healthy controls indicating that circulating DNA may also originate from other processes or comorbidities shared between the investigated groups. In contrast, histone citrullination is a process that is largely specific to NET formation[21] which has led us to conduct the first comprehensive biomarker analysis on citH3 in the AAA context. Patients and controls of our exploration set were well characterised and matched for age, sex, BMI and smoking habit, but they differed in AAA-related co-morbidities which are reportedly associated with NETosis.[10,22] Yet, in our exploration cohort, plasma citH3 was found to be significantly elevated in aneurysm patients vs controls, was not associated with co-morbidities but with anti-platelet and statin-based lipid-lowering therapy as previously described.[23] Furthermore, citH3 proved an independent parameter associated with AAA disease-state in multivariable analysis. The notion that citH3 levels might indicate AAA presence despite other co-morbidities with a known NET component was further supported by a validation set which included AAA patients and controls matched for pre-existing cardiovascular disease. Plasma citH3 levels differed significantly between groups. However, the specificity and sensitivity of circulating citH3 for AAA was substantially lower in the presence of cardiovascular comorbidity, indicating that the NET components may in part be originating from other atherosclerotic lesions.[24] There was limited added value when combining D-

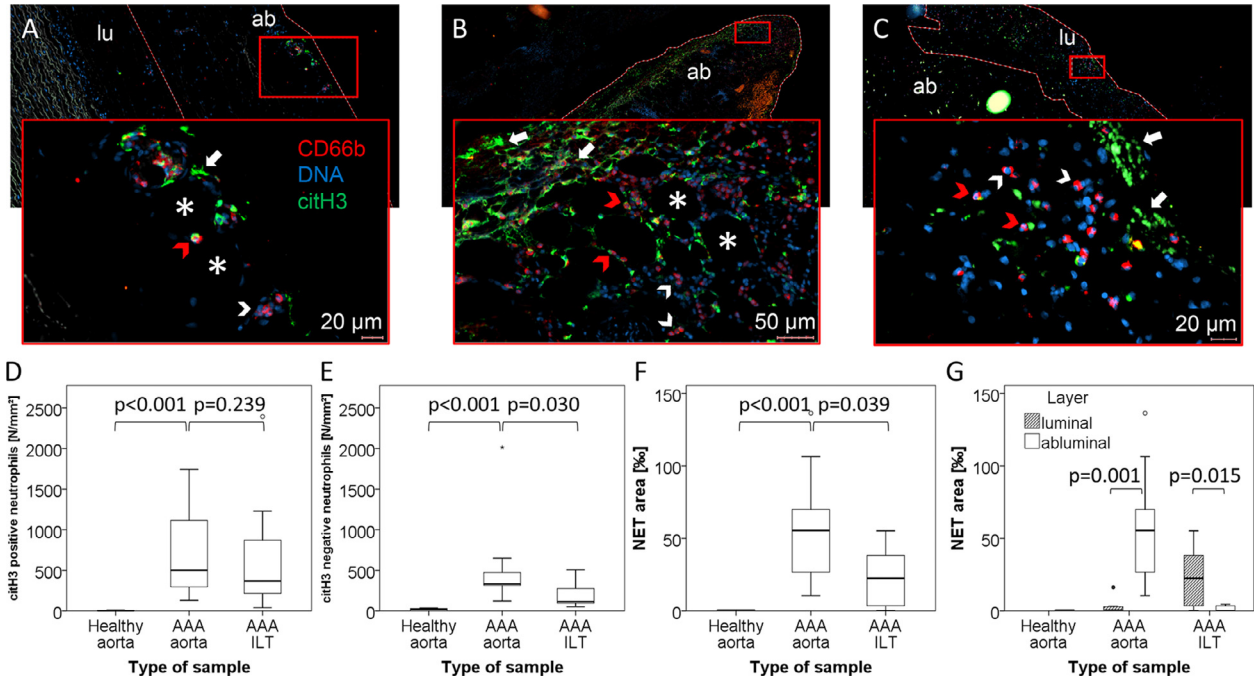

Fig 6. Analysis of neutrophils and NETs in aorta and ILT sections.

(A) Healthy aorta (N = 9), (B) AAA wall (N = 9) or (C) ILT (N = 7) sections were fluorescence-stained for CD66b (red) to detect granulocytes, for citH3 (green) and DNA (blue). Tissue images by TissueFAXS are given in overview and zoom-in region (white arrow heads: citH3 negative neutrophils, red arrow heads: citH3 positive neutrophils, white arrows: expelled NETs, white asterisks: lipid vacuoles in adventitia). Automated quantitation was based on TissueQuest software and data analysis by Mann-Whitney U test for (D) citH3 positive neutrophils, (E) citH3 negative neutrophils and (F) per-mille of NET area in scanned tissue. While the analyses in D-F focused on the luminal ILT and abluminal wall (adventitia), plot G compares luminal (lu) and abluminal (ab) layers of aortic wall (lu: contact side to ILT; ab: adventitia) and ILT (lu: contact side to blood; ab: contact side to vessel wall).

dimer and citH3 measurements in the diagnostic setting which supports the conclusion that NETs are involved in aberrant thrombus formation and turnover.[10] In line, plasma D-dimer ($r = 0.487$, $P < 0.001$, $N = 73$) and citH3 ($r = 0.296$, $P = 0.011$, $N = 73$) correlated with ILT volume rather than AAA diameter in our observation study.

The prognostic marker value of plasma citH3 for AAA. In the longitudinal monitoring study AAA patients (without indication for surgical repair) were followed at 6-month intervals by serial CTA and blood withdrawals. When patients were split into groups with slow and fast growth periods (corresponding to < 2 or ≥ 2 mm increase in CTA-determined AAA diameter over 6 months), baseline citH3 values exceeding 194 ng/mL predicted rapid aneurysm growth with 77% sensitivity and 64% specificity. While this is the first evaluation of plasma citH3 in AAA prognosis and warrants confirmation in a more comprehensive longitudinal study, the biomarker potential of citH3 to predict rapid disease progression (or possibly imminent rupture) would be of particular interest to clinical application, that is, patient stratification for early surgical repair.

The tissue-origin of circulating citH3 in AAA patients. Tissue investigations served to gather further proof for the presence and origin of citrullinated histones at the aneurysm site. The first indication came from the normalization of plasma citH3 levels after surgical repair. Histologically, the resected AAA tissue showed an abundance of NETosing neutrophils and formed NETs compared with their essential absence in healthy aortas. Of note, the analysis of tissue-conditioned medium indicated a higher citH3 level in ILT vs aneurysm wall, while NET prevalence was slightly lower in ILT compared to adventitia in histological sections. This discrepancy might relate to a better release of components from thrombus than aortic tissue into conditioned medium. Also, the histological analysis confirmed preceding reports demonstrating the predominance of NETs in the luminal region of the ILT and the abluminal (adventitial) part of the aorta, illustrating their route of entry.[11] Earlier attempts to detect citH3 in human AAA tissue homogenates or plasma by immunoblot failed, possibly due to sensitivity issues[12], but the prevalence of citH3 in AAA is now well documented and quantitated by the analyses of the present study.

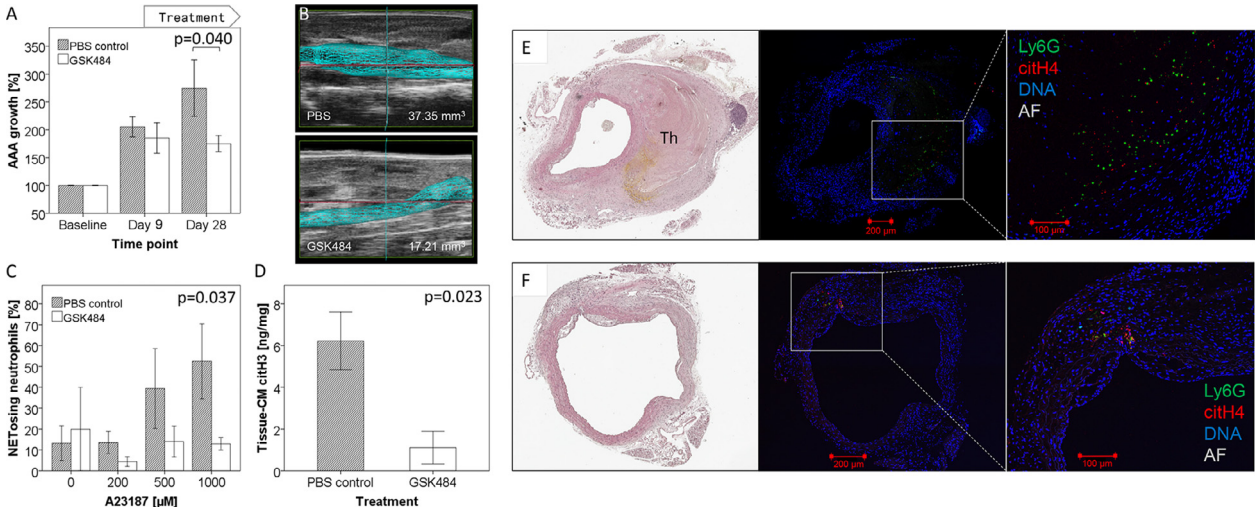

Fig 7. Inhibition of histone citrullination to block experimental AAA progression.

Aneurysms were induced by AngII administration to *ApoE* deficient mice over 28 days. On day 10, ports were implanted and daily injections of GSK484 (N = 8) or PBS (N = 8) were administered until day 28. (A) The suprarenal aortic volume was monitored by ultrasound and is given in % growth compared to baseline. Mice were stratified to treatment groups based on AAA volume of day 9 and statistical group comparison was performed on day 28 by paired T-test. (B) Two sample images of AAA volume calculations are shown. (C) On day 29, blood was harvested and challenged *ex vivo* with increasing doses of A23187. NET induction was evaluated by citH4 and Ly6G staining of blood smears. Data are shown as mean and standard error, the *p*-value refers to group difference over dose range in a linear mixed model with compound symmetric covariance. Aneurysms resected on day 29 were either subjected to (D) citH3 ELISA of tissue-conditioned medium (N = 5) or to (E,F) haematoxylin-eosin and immunofluorescence staining of suprarenal aorta sections for citH4 (red), Ly6G (green) and DNA (blue). (E) PBS-treated control showing a greatly enlarged and partly dissected aortic wall with an intramural thrombus (Th); (F) GSK484-treated mouse; note: weak autofluorescence (AF) of elastin and collagen fibres in white.

Preclinical evidence for targeting histone citrullination to block AAA progression. Regarding animal models, previous studies addressed the role of NETs in AAA initiation and characterised the potential triggers and downstream mediators. Thus, periodontal pathogens[11] and the central inflammatory mediator IL-1β[12] were revealed as activators of NET formation at the AAA site, and the propagation of chronic inflammation by NETs was described in rodent models.[13] The association between IL-1β and citH3 in NETs was also reflected by parameter correlations in our human tissue samples. Our experimental mouse model was designed to take NET targeting a step closer to clinical application in AAA. Rather than dismantling expelled NETs by DNase I[13] or preventing NET formation by pleiotropic agents against inflammation[14] and overall protein citrullination[12], we applied the specific PADI4 inhibitor GSK484 to selectively interfere with histone citrullination as a distinct hallmark of NETosis.[9] In line, GSK484 was well tolerated in mice at doses up to 100-fold of the finally applied treatment (data not shown) indicating that PADI4 inhibition exhibits a low toxicity and limited off-target profile. Also, mice deficient in NET formation do not show severe impairment of microbial clearance but rather a delay in the elimination of distinct pathogens which supports the notion of long-term NET inhibition.[21] Importantly, while all previous studies interfered with AAA formation by early-on or continuous drug administration starting at aneurysm initiation, we addressed disease progression rather than AAA formation in a mouse model to reproduce the clinical setting of established disease.

The therapeutic potential of targeting histone citrullination in AAA was evaluated using the well-established mouse model of angiotensin II-induced aneurysm formation in *ApoE* deficient mice. Aneurysms were allowed to develop before GSK484 application. While this AAA model comes with a 40%–50% rupture rate within the first 10 days, we did not experience animal loss during treatment phase, as mice were randomised and therapy was started by day 10. We could further limit the number of animals required for statistically meaningful results by conducting an ultrasound-based automated scan of the suprarenal aorta as opposed to the more commonly applied single-site assessment of maximal aortic diameter (in ultrasound analysis or on resected aneurysms). We found the interobserver variability of aortic volume analysis to be particularly low with a mean coefficient of variation of 7.4% (SD 5.1%) for 3 independent observers which allowed us to reliably detect also moderate increases in aortic expansion by day 9 and 28. Importantly, in this setting the inhibition of histone citrullination

was found to be effective in preventing further AAA growth. These are particularly appealing preclinical leads since conservative treatment options limiting AAA progression and avoiding surgical intervention are currently missing.

We would like to note, however, that GSK484 administration to established aneurysms in a second mouse model of AAA induced by elastase did not block disease progression despite the detectable presence of NET markers (Suppl. Figure 3). As this model relies on an acute inflammatory insult and differs substantially in pathogenesis from the angiotensin II-induced aneurysm formation in *ApoE* deficient mice, NETs might play a more crucial role in AAA initiation as opposed to progression in this setting. This notion is supported by the findings of Yan *et al.* who reported that DNase I application to dismantle NETs largely abrogated aneurysm formation in the mouse model of elastase perfusion when DNase I was given within the first 3 days of disease development, but was ineffective when administered thereafter.[13] To address the possibility that our novel approach of semi-automated 3D reconstruction and quantitation of the aortic volume over a stretch of 12 mm as opposed to the commonly assessed maximal aortic diameter might account for the negative results, we compared volume data with ultrasound-guided diameter as well as *ex vivo* measurements of external aortic diameter and found a high degree of correlation (Suppl. Figure 3). These data argue against a methodological error but rather indicate a difference in the NET-dependence of AAA progression in the 2 mouse models. Considering that the pathogenic triggers of the angiotensin II-driven model are closer to human risk factors for AAA and in view of the detectable abundance of NETs in human aneurysm tissue, therapeutic NET targeting may indeed constitute a promising approach for clinical AAA drug development.

CONCLUSIONS

Citrullinated histones are a hallmark of NET formation and abundantly detected in AAA tissue where NETs contribute to chronic inflammation. This study has evaluated the clinical potential of citH3 as a plasma biomarker and therapeutic target in AAA. Blood levels of citH3 were found to indicate the presence of an aneurysm but are also influenced by other cardiovascular morbidities. In particular, our data suggest that plasma citH3 holds prognostic potential to predict rapid AAA growth. Regarding therapeutic application, progression of an established aneurysm was blocked by a selective inhibitor of histone citrullination in a mouse model of angiotensin II-induced aneurysm formation in *ApoE* deficient mice.

LIMITATIONS OF THE STUDY

A self-composed ELISA was applied which has been used in several previous studies on human plasma samples.[17,25] While a commercial citH3 ELISA test is available (Cayman Chemical), its sensitivity is substantially lower compared to the self-composed ELISA and hence the majority of human plasma signals are at or below detection limit. Therefore, we have given preference to the self-composed ELISA despite limited inter-laboratory comparability.

Furthermore, we conducted MPO-DNA ELISA measurements for comparison, since cell-free MPO-DNA complexes are considered another hallmark of NET formation.[26,27] We found ELISA protocols (published for plasma analysis) to be sensitive and specific for *in vitro* generated NETs. Yet, in our experience these assays yield unspecific signals for plasma samples, as revealed when replacing the capture antibody by an isotype control (manuscript in preparation). Hence, we did not include data on MPO-DNA complexes in this manuscript.

The citH3 evaluation for prognostic marker value has been conducted on a limited data set from 28 patients with mostly 1-2 observation periods of 6 months. Hence, statistical analysis was based on group comparison of slow vs fast progression ($</\geq$ 2 mm/6 months) at a statistically meaningful sample size. Given the encouraging results, validation in an independent, prospective monitoring study is indicated which should cover longer monitoring periods and a longitudinal evaluation by linear mixed model or Cox hazard model.

With respect to mouse models of AAA formation, an inducible, myeloid-specific deletion of PADI4 on an *ApoE* deficient background would constitute a valuable tool to further investigate the role of histone citrullination in AAA progression in follow-up studies.

ACKNOWLEDGEMENTS

We would like to thank Sabine Rauscher, Marion Gröger (Core Facility Imaging) for help in Tissue-FAXS analysis, Alexandra Kaider and Robin Ristl (Centre for Medical Statistics) for statistics instructions, Prof. Podesser's team (Dept. of Biomedical Research, Medical University of Vienna) for assistance in animal experiments. We are grateful to Prof. Sven Brandau (University of Duisburg-Essen) for support in mouse immunohistochemistry and Laura Brunnthaler

(Dept. of Vascular Biology and Thrombosis Research, Medical University of Vienna) for MPO co-stainings of human AAA sections.

All authors have read the journal's authorship agreement and the manuscript has been reviewed by and approved by all named authors.

Conflicts of Interest: All authors have read the journal's policy on disclosure of potential conflicts of interest and have none to declare.

This work was supported by the Austrian Science Fund [SFB project F 5409-B21] as well as the Medical Scientific Fund of the Mayor of the City of Vienna, Austria [project 15012] and The Garfield Weston Foundation (for the Leeds Aneurysm Development Study, United Kingdom). Marc Bailey is personally supported by the British Heart Foundation [FS/18/12/33270]. The sponsors had no role in study design, the collection, analysis and interpretation of data; in the writing of the report; or in the decision to submit the article for publication.

SUPPLEMENTARY MATERIALS

Supplementary material associated with this article can be found, in the online version, at doi:10.1016/j.trsl.2021.02.003.

REFERENCES

1. Moll FL, Powell JT, Fraedrich G, et al. Management of abdominal aortic aneurysms clinical practice guidelines of the European society for vascular surgery. Eur J Vasc Endovasc Surg 2011;41 (Suppl 1):S1–s58.
2. Darling RC, Messina CR, Brewster DC, Ottinger LW. Autopsy study of unoperated abdominal aortic aneurysms. The case for early resection. Circulation 1977;56:II161–4.
3. Golledge J, Muller R, Clancy P, McCann M, Norman PE. Evaluation of the diagnostic and prognostic value of plasma D-dimer for abdominal aortic aneurysm. Eur Heart J 2011;32:354–64.
4. Zagrapan B, Eilenberg W, Prausmueller S, et al. A novel diagnostic and prognostic score for abdominal aortic aneurysms based on D-dimer and a comprehensive analysis of myeloid cell parameters. Thromb Haemost 2019;119:807–20.
5. Michel JB, Martin-Ventura JL, Egido J, et al. Novel aspects of the pathogenesis of aneurysms of the abdominal aorta in humans. Cardiovasc Res 2011;90:18–27.
6. Piechota-Polanczyk A, Jozkowicz A, Nowak W, et al. The Abdominal Aortic Aneurysm and Intraluminal Thrombus: Current Concepts of Development and Treatment. Front Cardiovasc Med 2015;2:19.
7. Eliason JL, Hannawa KK, Ailawadi G, et al. Neutrophil depletion inhibits experimental abdominal aortic aneurysm formation. Circulation 2005;112:232–40.
8. Brinkmann V, Reichard U, Goosmann C, et al. Neutrophil extracellular traps kill bacteria. Science 2004;303:1532–5.
9. Lewis HD, Liddle J, Coote JE, et al. Inhibition of PAD4 activity is sufficient to disrupt mouse and human NET formation. Nat Chem Biol 2015;11:189–91.
10. Martinod K, Wagner DD. Thrombosis: tangled up in NETs. Blood 2014;123:2768–76.
11. Delbosc S, Alsac JM, Journe C, et al. Porphyromonas gingivalis participates in pathogenesis of human abdominal aortic aneurysm by neutrophil activation. Proof of concept in rats. PLoS One 2011;6:e18679.
12. Meher AK, Spinosa M, Davis JP, et al. Novel role of IL (interleukin)-1beta in neutrophil extracellular trap formation and abdominal aortic aneurysms. Arterioscler Thromb Vasc Biol 2018;38:843–53.
13. Yan H, Zhou HF, Akk A, et al. Neutrophil proteases promote experimental abdominal aortic aneurysm via extracellular trap release and plasmacytoid dendritic cell activation. Arterioscler Thromb Vasc Biol 2016;36:1660–9.
14. Spinosa M, Su G, Salmon MD, et al. Resolvin D1 decreases abdominal aortic aneurysm formation by inhibiting NETosis in a mouse model. J Vasc Surg 2018;68:93S–103S.
15. Parry DJ, Al-Barjas HS, Chappell L, Rashid ST, Ariens RA, Scott DJ. Markers of inflammation in men with small abdominal aortic aneurysm. J Vasc Surg 2010;52:145–51.
16. Starlinger P, Moll HP, Assinger A, et al., et al. Thrombospondin-1: a unique marker to identify in vitro platelet activation when monitoring in vivo processes. J Thromb Haemost 2010;8:1809–19.
17. Thalin C, Daleskog M, Goransson SP, et al. Validation of an enzyme-linked immunosorbent assay for the quantification of citrullinated histone H3 as a marker for neutrophil extracellular traps in human plasma. Immunol Res 2017;65:706–12.
18. Lu H, Howatt DA, Balakrishnan A, et al. Subcutaneous Angiotensin II Infusion using Osmotic Pumps Induces Aortic Aneurysms in Mice. J Vis Exp 2015.
19. Gandhi R, Cawthorne C, Craggs LJL, et al. Cell proliferation detected using [^{18}F]FLT PET/CT as an early marker of abdominal aortic aneurysm. J Nuclear Cardiol 2019. https://doi.org/10.1007/s12350-019-01946-y Epub ahead of print. PMID: 31741324.
20. Vega de Ceniga M, Gomez R, Estallo L, Rodriguez L, Baquer M, Barba A. Growth rate and associated factors in small abdominal aortic aneurysms. Eur J Vasc Endovasc Surg 2006;31:231–6.
21. Wong SL, Wagner DD. Peptidylarginine deiminase 4: a nuclear button triggering neutrophil extracellular traps in inflammatory diseases and aging. FASEB J 2018:fj201800691R.
22. Franck G, Mawson TL, Folco EJ, et al. Roles of PAD4 and NETosis in Experimental Atherosclerosis and Arterial Injury: Implications for Superficial Erosion. Circ Res 2018;123:33–42.
23. Chow OA, von Kockritz-Blickwede M, Bright AT, et al. Statins enhance formation of phagocyte extracellular traps. Cell Host Microbe 2010;8:445–54.
24. Megens RT, Vijayan S, Lievens D, et al. Presence of luminal neutrophil extracellular traps in atherosclerosis. Thromb Haemost 2012;107:597–8.
25. Mauracher LM, Posch F, Martinod K, et al. Citrullinated histone H3, a biomarker of neutrophil extracellular trap formation, predicts the risk of venous thromboembolism in cancer patients. J Thromb Haemost 2018;16:508–18.
26. Guy A, Favre S, Labrouche-Colomer S, et al. High circulating levels of MPO-DNA are associated with thrombosis in patients with MPN. Leukemia 2019;33:2544–8.
27. Lood C, Blanco LP, Purmalek MM, et al. Neutrophil extracellular traps enriched in oxidized mitochondrial DNA are interferogenic and contribute to lupus-like disease. Nat Med 2016;22:146–53.